



Efficient valorization of biomass-derived furfural to fuel bio-additive over aluminum phosphate

Fang, Wenting; Riisager, Anders

Published in:
Applied Catalysis B: Environmental

Link to article, DOI:
[10.1016/j.apcatb.2021.120575](https://doi.org/10.1016/j.apcatb.2021.120575)

Publication date:
2021

Document Version
Publisher's PDF, also known as Version of record

[Link back to DTU Orbit](#)

Citation (APA):
Fang, W., & Riisager, A. (2021). Efficient valorization of biomass-derived furfural to fuel bio-additive over aluminum phosphate. *Applied Catalysis B: Environmental*, 298, Article 120575.
<https://doi.org/10.1016/j.apcatb.2021.120575>

General rights

Copyright and moral rights for the publications made accessible in the public portal are retained by the authors and/or other copyright owners and it is a condition of accessing publications that users recognise and abide by the legal requirements associated with these rights.

- Users may download and print one copy of any publication from the public portal for the purpose of private study or research.
- You may not further distribute the material or use it for any profit-making activity or commercial gain
- You may freely distribute the URL identifying the publication in the public portal

If you believe that this document breaches copyright please contact us providing details, and we will remove access to the work immediately and investigate your claim.



Efficient valorization of biomass-derived furfural to fuel bio-additive over aluminum phosphate

Wenting Fang, Anders Riisager *

Centre for Catalysis and Sustainable Chemistry, Department of Chemistry, Technical University of Denmark, DK-2800, Kgs. Lyngby, Denmark

ARTICLE INFO

Keywords:

Aluminum phosphate
Acetalization
Reductive etherification
Biomass valorization
Fuel bio-additive

ABSTRACT

Aluminum phosphates (APO-5s) were synthesized and evaluated as heterogeneous catalysts for the valorization of furfural to furfuryl acetals (FAs) and furfuryl alcohol ethers (FAEs). Weakly acidic APO-5 (Al/P = 1) exhibited excellent catalytic performance with 96 % FA yield in ethylene glycol, and analysis of the acetalization reaction supported that adsorption and acidic catalyst sites co-catalyzed the reaction. In addition, the catalyst was stable and reusable though with some deactivation after five recycles. Oppositely, more acidic APO-5 (Al/P = 1.5) catalyzed the one-pot synthesis of FAE with 55 % yield in 2-propanol with unchanged performance in three successive reactions after intermediate calcination. The reaction pathway for the direct hydrogenolysis of acetal into ether by catalytic transfer hydrogenation and etherification was promoted by the co-solvent 1,4-dioxane, possibly by hydrogen bonding. The study demonstrates a simple approach to design APO catalyst systems allowing very efficient and highly selective valorization of furfural to fuel bio-additives.

1. Introduction

In the last century, the World's energy demand has predominantly been covered by nonrenewable carbon-based fossil fuels, which are gradually becoming exhausted. This has led to severe environmental problems such as global warming, and uncertainty about future supply safety. Accordingly, great efforts have been undertaken to develop potential substitutes to fossil fuels. Biofuels, which are obtained from biomass, are renewable and environmental friendly alternatives to fossil fuels [1]. Biofuels can either be used directly or mixed in fossil fuels as bio-additives to improve the cetane number, density, cloud point, flash point or other fuel properties [2–4].

Furfural (FF) has been emphasized as one of the top value-added chemicals derived from biomass and can be widely used to produce different other chemicals [5]. Especially bio-additives derived from FF by acetalization (furfuryl acetals, FAs) and reductive etherification (furfuryl alcohol ethers, FAEs) have attracted attention due to their potential as blending high-octane gasoline components [6–10]. Formation of cyclic FAs from FF and diols can be obtained using various heterogeneous acid catalysts, where the pore structure and nature of the acid sites can be important [11,12]. Hence, ZSM-5 zeolite converted 35 % of FF with 100 % selectivity to FA in 1,2-propanediol [13], whereas sulfated-SnO₂ allowed to obtain a total yield of 82 % of 1,3-dioxolane

and 1,3-dioxane isomers in glycerol [14]. Moreover, Zr-Montmorillonite catalyzed the conversion of FF in different C₂-C₆ diols to the corresponding cyclic FAs with yields above 75 %, and particularly the products with ethylene glycol (EG) and 1,5-pentanediol were shown to exhibit high miscible in commercial diesel obtaining improved density, cloud point and flash point [15]. Similarly, FAEs are typically synthesized from acid-catalyzed direct etherification of furfuryl alcohol (FAL) [8,16,17], and furfuryl ethyl ether (EMF) have been noted for its excellent property to curb soot emissions and shows superior anti-knocking properties compared to the reference Euro 95 gasoline [18,19]. Recently, Sn-beta and Zr-TUD-1 zeotype catalysts were applied for one-pot formation of furfuryl butyl ether (BMF) from FF allowing to obtain 58 % BMF yield with 95 % FF conversion and 25 % BMF yield with 87 % FF conversion, respectively [20,21].

In this work, aluminum phosphate (APO-5) catalysts with different Al/P ratios were synthesized by hydrothermal method, characterized by multiple techniques and applied for acetalization and reductive etherification of FF. Weakly acidic APO-5(1) showed excellent catalytic performance and high stability for FF acetalization with EG. The active sites of the catalyst were investigated, and the reaction evaluated with respect to substrate and solvent scope. More acidic APO-5(1.5) exhibited high activity for the one-pot synthesis of FAE from FF in 2-propanol, and isotopic tracing study provided insight to the reaction pathway. The

* Corresponding author.

E-mail address: ar@kemi.dtu.dk (A. Riisager).

<https://doi.org/10.1016/j.apcatb.2021.120575>

Received 15 April 2021; Received in revised form 26 July 2021; Accepted 28 July 2021

Available online 31 July 2021

0926-3373/© 2021 The Author(s). Published by Elsevier B.V. This is an open access article under the CC BY license (<http://creativecommons.org/licenses/by/4.0/>).

reusability of the spent catalysts was examined by catalytic as well as characterization studies.

2. Experimental

2.1. Materials

Phosphoric acid 85 % (H_3PO_4 , $\geq 99.8\%$), aluminum isopropoxide (Al(O-*i*-Pr) $_3$, $\geq 98\%$), triethylamine (Et_3N , $\geq 99\%$), furfural (FF, 99 %), furfuryl alcohol (FAL, 98 %), methanol ($\geq 99.9\%$), ethanol ($\geq 99.8\%$), 1-propanol ($\geq 99.9\%$), 2-propanol ($\geq 99.5\%$), 1-butanol ($\geq 99.4\%$), 2-butanol (99.5 %), *iso*-butanol (99.5 %), 1,4-dioxane (99.8 %), ethylene glycol (EG, 99.8 %), 1,2-propanediol ($\geq 99.5\%$), 1,3-propanediol (98 %), glycerol (99.5 %), 1,4-butanediol (99 %), 1,5-pentanediol ($\geq 97\%$), 1,6-hexanediol (97 %), methanol- d_4 ($\geq 99.8\%$), 5-hydroxymethylfurfural (HMF, $\geq 99\%$), 5-methylfurfural (MFA, 99 %), 2,5-furandicarboxaldehyde (FCA, 97 %), dimethyl sulfoxide (DMSO, $\geq 99.9\%$), and decane ($\geq 99\%$) were purchased from Sigma-Aldrich while 2-propanol-OD ($> 98\%$) was purchased from Apollo Scientific Ltd. All chemicals were used as received.

2.2. Catalyst synthesis

The APO-5 catalysts were prepared as described elsewhere [22] using a gel composition of 1~1.5 Al_2O_3 :1 P_2O_5 :1 Et_3N :45 H_2O . Al(O-*i*-Pr) $_3$ (14.30 g~21.45 g, 0.07 mol~0.105 mol) was added to 23 mL distilled water and the mixture vigorously stirred for 0.5 h. Then a solution of 85 % H_3PO_4 (8.07 g, 0.07 mmol) in 5 mL distilled water was added dropwise and the resulting solution stirred for 2 h. Subsequently, Et_3N (4.9 mL) was added slowly followed by stirring for another 1 h where after the solution was transferred to an autoclave, which was tightly closed and kept at 175 °C under autogeneous pressure for 48 h. After reaction, the autoclave was cooled to room temperature and the obtained product washed with distilled water several times, oven dried at 110 °C for 12 h and finally calcined at 550 °C for 7 h.

APO-5 with Al/P = 1, 1.25 and 1.5 were denominated as APO-5(1), APO-5(1.25) and APO-5(1.5), respectively. APO-5(1.5) without calcination was denominated as UC/APO-5(1.5).

2.3. Catalyst characterization

Powder X-ray diffraction (XRD) was performed on a Huber G670 diffractometer with Cu- $\text{K}\alpha$ radiation ($\lambda = 0.154056$ nm) with 2θ ranging from 3 to 100°.

Brunauer-Emmett-Teller (BET) surface area and porosity analysis were evaluated by N_2 physisorption performed at -196 °C by a Micromeritics ASAP 2020 instrument. The samples were degassed at 250 °C for 4 h before the measurement.

X-ray fluorescence (XRF) spectra were measured on a PANalytical epsilon3-XL instrument. Samples were prepared by fusing them into disks using a Claisse LeNeo fluxer oven.

Ammonia temperature-programmed desorption (NH_3 -TPD) were performed on a Micromeritics AutoChem II 2920 apparatus to determine the acid properties of the samples. Initially, the samples (100 mg) were exposed to He gas flow (25 cm^3/min) and heated up to 600 °C followed by cooling to 100 °C. Then NH_3 adsorption was carried out by purging with 1 vol.% NH_3/He gas mixture for 1 h, where after physically adsorbed gas was removed by purging with He gas for 1 h. Desorption of NH_3 was eventually conducted in the temperature range 100–600 °C with a heating ramp of 10 °C/min and the amount of liberated gas quantified by a thermal conductivity detector (TCD) and calibration curves.

Fourier-transform infrared (FT-IR) spectra of fresh and used catalysts as well as catalysts with pre-adsorbed additives were recorded on a NICOLET iS50 (Thermo) spectrometer equipped with an iS50 attenuated total reflectance (ATR) attachment. The catalysts with adsorbed FF and

other additives were prepared by the following method before the measurements: Catalyst (50 mg), FF (48 mg, 0.5 mmol), additive (50 mg) and methanol (1 mL) were mixed and shaken vigorously for 5 min followed by oven drying at 80 °C for 2 h to remove the methanol.

Scanning electron microscopy (SEM) images of samples were recorded on an AFEG 250 Analytical ESEM at 5 kV.

Thermogravimetric (TG) analysis of samples was conducted under air flow from 25 to 800 °C on a Mettler Toledo thermal analyzer with 10 °C/min heating rate.

^{27}Al and ^{31}P magic-angle spinning nuclear magnetic resonance (MAS NMR) spectra were recorded on a Bruker AVANCE III HD spectrometer operating at a magnetic field of 14.05 T equipped with a 4 mm CP/MAS BBFO probe.

2.4. Catalyst activity tests

The acetalization and reductive etherification of FF were conducted in 15 mL ACE pressure tubes in an oil bath with a magnetic stirrer. A mixture of FF (96 mg, 1 mmol) catalyst (100 mg), and solvent (5 mL) was added to the tube and the tube placed in an oil bath with a designated reaction temperature. After a specified reaction time, the tube was cooled to room-temperature and liquid samples of the reaction mixture were analyzed. The reaction solution after FF acetalization was analyzed using DMSO as an internal standard by ^1H NMR (Bruker 400 MHz spectrometer, room temperature, methanol- d_4). The reaction solution after reductive etherification was analyzed using decane as an internal standard with gas chromatography-mass spectrometry (GC-MS) (Agilent 6850-5975C) using a flame-ionization detection (GC-FID) (Agilent 6890 N), both equipped with an HP-5MS capillary column (30.0 m \times 250 μm \times 0.25 μm). Acetalization and reductive etherification of other aldehydes were also performed according to the above procedures.

2.5. Catalyst recycling test

The reusability of APO-5(1) was examined for the acetalization of FF at 150 °C after 2 h reactions. After initial reaction, the catalyst was collected *via* centrifugation, washed with acetone and methanol twice (2 \times 10 mL), respectively, followed by drying at 80 °C for 2 h before being used in the next reaction run. The reusability of APO-5(1.5) was evaluated for the reductive etherification of FF at 140 °C in 24 h reactions. Since APO-5(1.5) showed deactivation after applying the same washing protocol used for APO-5(1), the catalyst was calcined in air at 550 °C for 1 h after the third run before being used in the next run.

3. Results and discussion

3.1. Characterization of APO-5 catalysts

The XRD patterns (Fig. 1a) of the APO-5 catalysts matched well with the AFI structure [23,24]. APO-5(1) exhibited the best crystallinity among the three samples, while a very broad and weak peak occurred for APO-5(1.25) and APO-5(1.5) in the 2θ range of 15–30°. The Al source (Al(O-*i*-Pr) $_3$) was calcined at the same conditions as the catalysts and analyzed by XRD (Fig. S1). The broad and weak peak found matched with the peak of the calcined Al source, indicating that some amorphous extra-framework Al species was formed when the Al concentration was increased [25].

The N_2 adsorption-desorption isotherms of the APO-5 catalysts are shown in Fig. 1b. APO-5(1) displayed type I isotherms indicative of a microporous structure in consistence with previous data [26]. In contrast, APO-5(1.25) and APO-5(1.5) exhibited type IV isotherms typical of mesoporous materials with H3 type hysteresis loops in the region $0.7 < P/P_0 < 0.95$. The BET surface area of APO-5(1.5) (236 m^2/g) was close to that of APO-5(1) (197 m^2/g), but the mesopore volume of the former (0.51 cm^3/g) was nearly six times larger than the latter (0.09 cm^3/g) (Table 1). The pore size distribution analysis showed

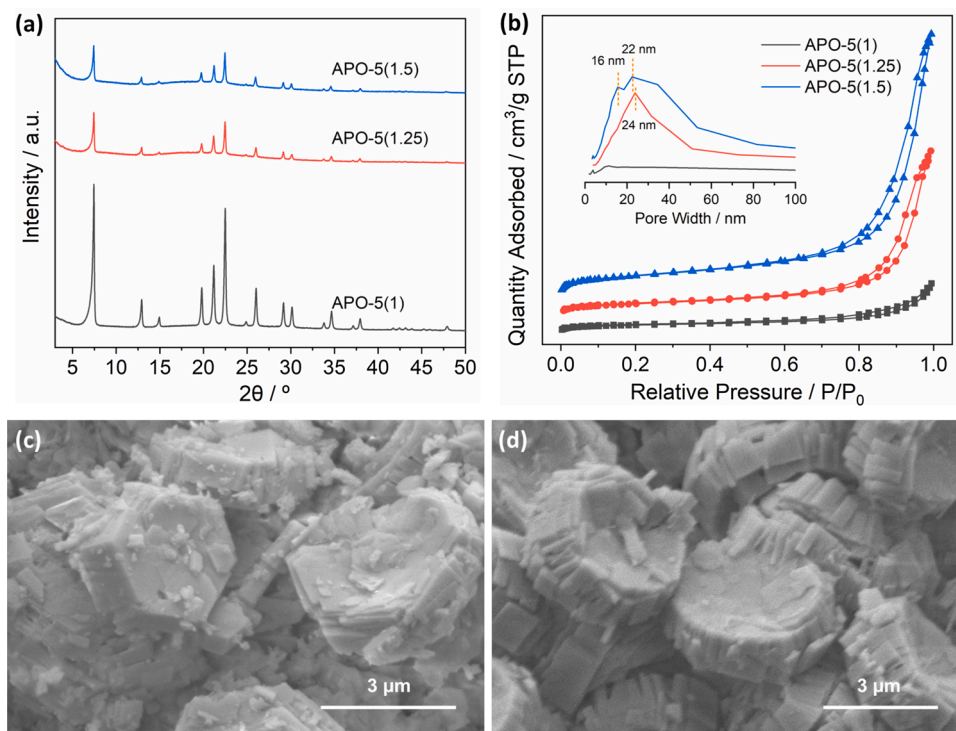


Fig. 1. (a) XRD patterns and (b) N_2 adsorption-desorption isotherms (inset: BJH mesopore size distribution) of APO-5 catalysts. (c) SEM image of APO-5(1) and (d) SEM image of APO-5(1.5).

Table 1
Textural properties of the APO-5 catalysts

Sample	Al/P molar ratio ^a	S_{BET} (m ² /g) ^b	V_{micro} (cm ³ /g) ^c	V_{meso} (cm ³ /g) ^d	Acidity (mmol/g) ^e
APO-5(1)	0.95	197	0.07	0.09	0.0012
APO-5(1.25)	1.19	177	0.04	0.32	0.29
APO-5(1.5)	1.43	236	0.04	0.51	0.40

^a Determined by XRF.

^b Calculated by the BET method.

^c Estimated by the t-plot method.

^d Calculated by subtraction of the micropore volume from the total pore volume.

^e Determined by NH_3 -TPD.

mesopores in APO-5(1.25) of 24 nm, while APO-5(1.5) had mesopores of both 16 and 22 nm, which may be formed by the accumulation of amorphous Al species [27]. In addition, the mesopore volume of APO-5(1.5) before calcination (UC/APO-5(1.5)) was much larger than that of APO-5(1) (Table 1, entry 1, Table S1, entry 1 and Fig. S2), indicating that the mesoporosity predominantly originated from aggregation of Al species and only partly from the organic template [27].

From the SEM images of APO-5(1) and APO-5(1.5) (Fig. 1c and d), the particle sizes were found to be 4–5 μm which is normal sizes for APO-5 crystallites [28,29]. APO-5(1) had a hexagon prism-like shape, while the particles appeared as spherical plates in APO-5(1.5). This change in morphology may be a result of different pH of the gels during synthesis [29,30]. The cracks observed in the particles of APO-5(1.5) may contribute to the meso- and macroporosity obtained from the N_2 adsorption-desorption isotherms (Table 1).

To investigate the coordination environment of phosphorus and aluminum in the APO-5 samples, solid-state MAS NMR spectroscopy was performed. The ^{31}P MAS NMR spectra (Fig. 2a) revealed a characteristic broad asymmetric signal at -26 ppm with a shoulder at around -20 ppm

associated to $P(OAl)_4$, as also found in previous reports [31,32]. The signal at -26 ppm is assigned to fully crystallized $P(OAl)_4$, while the signal at -20 ppm corresponds to a semicrystalline phase which continuously evolve to the fully crystalline phase [31,33]. Higher Al concentration in the APO-5s led to a larger peak intensity at -20 ppm, suggesting that APO-5(1) had the most stable structure. The ^{27}Al MAS NMR spectra of the catalysts (Fig. 2b) showed a signal at 41 ppm characteristic of tetrahedrally coordinated Al linked to four phosphorus atoms via bridging oxygen atoms ($Al(OP)_4$) [34]. Moreover, a signal at 10 ppm could according to literature be assigned to unreacted Al or pentacoordinated Al with four Al atoms and one water molecule ($P(OAl)_4(H_2O)$) [35–37]. However, FT-IR spectra of the samples (Fig. 2c) did not indicate water in the structure and XRD showed presence of amorphous Al, thus suggesting the signal belonging instead to extra-framework Al species. In the FT-IR spectra of APO-5, the strong band at around 1100 cm^{-1} is characteristic of an asymmetric P-O-Al stretching vibration [23], and the red shift of the band observed with higher Al/P ratio may be due to small structural differences caused by the increased amount of Al. The bands at 704 and 665 cm^{-1} are assigned to the symmetric stretching and bending mode vibrations of P-O-Al, respectively. The bands at 634 and 561 cm^{-1} are assigned to double-ring vibration modes, while the band located at 458 cm^{-1} can be assigned to the internal T—O bending mode vibration [23,38,39].

NH_3 -TPD profiles of the APO-5 samples are shown in Fig. 2d. APO-5(1) had only a small peak at 164 $^{\circ}C$, indicating a low amount of weak acid sites consistent with the assumption that APO-5 is neutral. In contrast, APO-5(1.25) and APO-5(1.5) had three major peaks at 170, 240 and 340 $^{\circ}C$ correspondingly assigned to weak, medium and strong acid sites (Table S2). The acidity of the catalysts increased with the Al concentration (Table 1), which in combination with the XRD and ^{27}Al MAS NMR results inferred that the acidity was likely ascribed to extra-framework Al species.

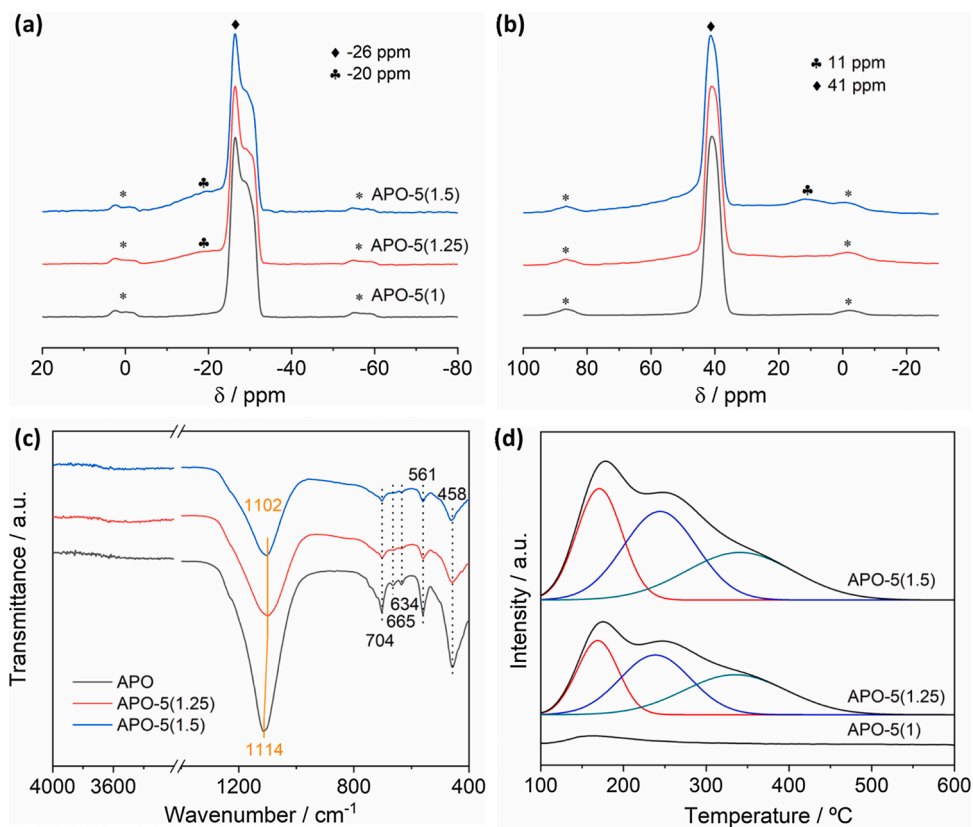


Fig. 2. (a) ^{31}P MAS NMR and (b) ^{27}Al MAS NMR spectra (* corresponds to spinning bands), (c) FT-IR spectra and (d) NH_3 -TPD profiles of APO-5 catalysts.

3.2. Catalytic performance of APO-5 catalysts

The APO-5 catalysts were initially screened for the catalytic conversion of FF in 2-propanol and the results are shown in Table 2. Interestingly, the APO-5 catalysts with diverse acidity showed different product selectivity. Obviously, APO-5(1) gave high acetalization selectivity towards 2-(diisopropoxymethyl)furan (DIPF) despite the reaction was completed in a solvent with high hydrogen-donor ability. In contrast, APO-5(1.5) exhibited a strong preference for hydrogen-transfer hydrogenation to FAL and the subsequent etherification to FAs, providing the possibility of one-pot formation of FAs with higher temperature where etherification is promoted [40]. Therefore, APO-5(1) and APO-5(1.5) were selected for further optimization of acetalization and reductive etherification of FF in different solvents, respectively.

3.3. Acetalization of furfural over APO-5(1)

3.3.1. Time course study

The acetalization of FF to 2-(furan-2-yl)-1,3-dioxane (FD) in EG/1,4-dioxane mixture using APO-5(1) was investigated as a representative

Table 2
Catalytic performance of APO-5 catalysts for FF conversion^a.

Catalyst	Conversion (%) ^b	Product Selectivity (%) ^b			
		FAL	DIPF	IPF	IPL
APO-5(1)	19.8	16.9	66.8	12.0	0.6
APO-5(1.25)	29.1	58.1	37.5	3.3	0.2
APO-5(1.5)	47.3	69.5	18.6	8.1	1.0

^a Reaction conditions: FF (96 mg, 1 mmol), catalyst (50 mg), 2-propanol (5 mL), 100 °C, 48 h.

^b Conversion and yield were quantified using GC. FAL: furfuryl alcohol; DIPF: 2-(diisopropoxymethyl)furan; IPF: 2-(isopropoxymethyl)furan; IPL: isopropyl levulinate.

reaction to demonstrate cyclic FA formation (Fig. 3). An excellent performance of the catalyst with FD selectivity >98 % throughout the reaction led to 97 % FF conversion and 96 % FD yield after 24 h. Moreover, both the FF conversion and FD yield remained very constant after 16 h of reaction (Fig. 3), indicating that FD remained stable under the condition.

To corroborate if furan-2-yl(hydroxymethoxy)methanol (I) was formed as an intermediate during the reaction, the product mixtures were analyzed by ex-situ ^1H NMR (Fig. S3). The aldehydic proton (d) of FF gradually disappeared while the acetalic proton (d') in FD appeared without indication of a hemiacetal intermediate being formed, thus implying that the formation of FD by water removal from (I) was most

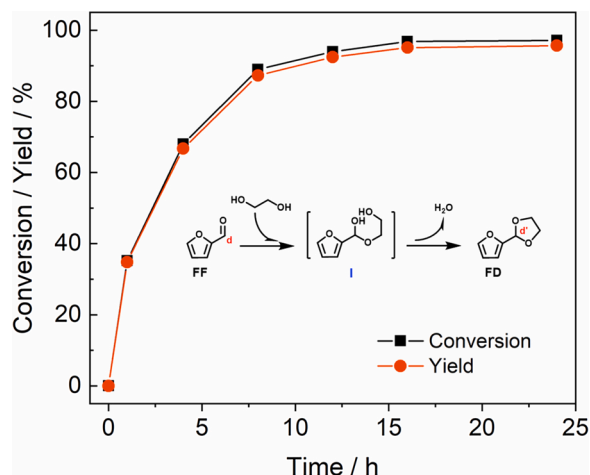


Fig. 3. FF conversion and FD yield at various reaction times during acetalization using APO-5(1). Reaction conditions: FF (96 mg, 1 mmol), APO-5(1) (100 mg), EG (2 mL), 1,4-dioxane (3 mL), 150 °C.

likely very fast. Notably, when the reaction was performed in neat EG instead of EG/1,4-dioxane mixture both the FF conversion and the FD selectivity were lowered significantly and 2,2'-(furan-2-ylmethylene)bis(oxy))bis(ethan-1-ol) formed (Table S3, entry 2), confirming that 1,4-dioxane improved both catalyst activity and selectivity.

3.3.2. Active site study

Acetalization is in literature reported to be an acid-catalyzed reaction [1,41]. Nevertheless, APO-5(1) having only few acid sites (0.0012 mmol/g) showed excellent catalytic performance in the acetalization of FF. Hence, in order to determine the role of acidity and basicity for the catalytic system pyridine, benzoic acid and 2,6-lutidine were separately introduced into the reaction as poisoning additives for acidic, basic and Brønsted acidic sites, respectively [42]. (Fig. 4a). In the presence of benzoic acid, the conversion of FF and yield of FD were almost unaffected while the addition of pyridine drastically reduced both FF conversion and FD yield, suggesting that the active centers of acetalization were acidic sites. Furthermore, when Brønsted acid sites were selectively poisoned by 2,6-lutidine the catalytic activity was suppressed even more than with pyridine, showing that Brønsted acid sites were the main active centers which is also in line with previous studies [13]. FT-IR spectra of APO-5(1) with adsorbed FF with or without poison additives were further recorded (Fig. 4b). Comparison of the C=O stretching bands of FF and FF adsorbed on APO-5(1) revealed a red shift from 1668 to 1663 cm^{-1} , indicating that the C=O group of FF adsorbed strongly on APO-5(1) [43,44], which may further lead to excellent activity of APO-5(1). Notably, an additional red shift of the band occurred after pyridine or 2,6-lutidine addition (1659 cm^{-1}), which combined with the results of the poisoning reactions inferred that the adsorption sites of FF were not the Brønsted acidic sites. Thus, the Brønsted acidic sites and alternative acidic FF adsorption sites probably together catalyzed the acetalization of FF in the system.

3.3.3. Catalyst recycling study

The recyclability of the APO-5(1) catalyst was studied for the acetalization of FF to FD after reaction at 150 °C for 2 h (Fig. 4c). During five consecutive reaction cycles, the FD yield reduced from 57.9 to 44.1% whereas a high constant FD selectivity of 98–99 % was maintained, clearly indicating that only a minor part of the active centers were clogged. XRD analysis of the spent catalyst confirmed that its structure was intact after the reaction cycles (Fig. S4), while N_2 physisorption analysis revealed significant reductions of surface area and microporous volume compared to the fresh catalyst (Table 1, entry 1 and Table S1, entry 2), implying that micropores were blocked. Therefore, most of the active sites were not in the micropores. In line with this, TG analysis of the recovered catalyst (Fig. S5) gave new peaks at 297 and 450 °C ascribed to adsorbed organic species (9.3 wt.%), which were likely responsible for the deactivation of the catalyst. Also new bands formed in the FT-IR spectra (Fig. S6) around 2900 and 1400 cm^{-1} (C–H stretching and bending vibrations of CH_3 and CH_2) demonstrated remnant of organic species (bands at 1220 and 870 cm^{-1} attributed to

adsorption of 1,4-dioxane [45]).

3.3.4. Substrate and solvent scope study

As the APO-5(1) catalyst exhibited remarkable activity in the acetalization of FF to FD in EG, the study was expanded to acetalization of other furanic carbonyl compounds like FCA, MFA and HMF (Table 3). All substrates were efficiently converted to the corresponding acetals, but FCA with two carbonyl groups required probably longer reaction time to reach high yield (Table 3, entry 2), and the hydroxy group of HMF etherified with EG and formed side product (Table 3, entry 4). Cyclic acetalization of FF in alternative C_3 – C_6 diols was also evaluated (Table S3). The APO-5(1) catalyst revealed also here high activity in especially 1,2-propanediol and 1,3-propanediol giving around 90 % yields of the corresponding cyclic acetals, whereas the total yield of acetal isomers in glycerol was above 70 % which is similar to previous work [11]. However, with increasing diol chain length the yield of FA and the conversion of FF became lower likely because the pore size of the catalyst limited the acetalization reaction of the larger sized diols.

3.4. Reductive etherification of furfural over APO-5(1.5)

3.4.1. Time course study

In order to investigate the reductive etherification of FF in 2-propanol a time course was completed at 120 °C for 70 h (Fig. 5a). During the reaction, FF was gradually converted (>95 % after 50 h) into a mixture of mainly FAL by hydrogenation, IPF by consecutive etherification of FAL and IPL by continuous hydrolysis of IPF, respectively. Additionally, a minor amount of the acetal intermediate DIPF formed in the beginning of the reaction, but was gradually converted along with the consumption of FF either by reversible hydrolysis of the formed DIPF (pathway a) [46–48] or by direct hydrogenolysis of DIPF as previously indicated possible in literature (pathway b) [9,49].

In Scheme 1, two possible mechanisms for the formation of IPF (from DIPF) via pathways A and B are proposed. To investigate if both reaction pathways occurred with APO-5(1.5), isotopic tracing experiments in deuterated 2-propanol, $\text{CH}_3\text{CH}(\text{OD})\text{CH}_3$ (2-PrOD), followed by GC–MS analysis were performed (Fig. 5c and d). With unlabeled 2-propanol (2-PrOH) as solvent, the MS fragments of the FAL and IPF products provided the parent ions m/z 97, 98 and 99 and m/z 140, 141 and 142, respectively, in relative ratios which was the same as obtained in a reference reaction without catalyst (as expected). However, using 2-PrOD as solvent, the ratio (34.4 %) of FAL with the ion m/z 99 was much higher than that of the reference reaction (4.6 %). This indicated replacement of a hydrogen atom in the molecule with deuterium, thus supporting an intermolecular hydrogen-transfer mechanism from 2-propanol to FF [42]. For the IPF product, the intensity of the ion m/z 140 was also reduced, but to a lower extent, while the intensities of the ions m/z 141 and 142 were increased correspondingly. This indicated that IPF formation also partly occurred by hydrogenolysis via pathway B [49].

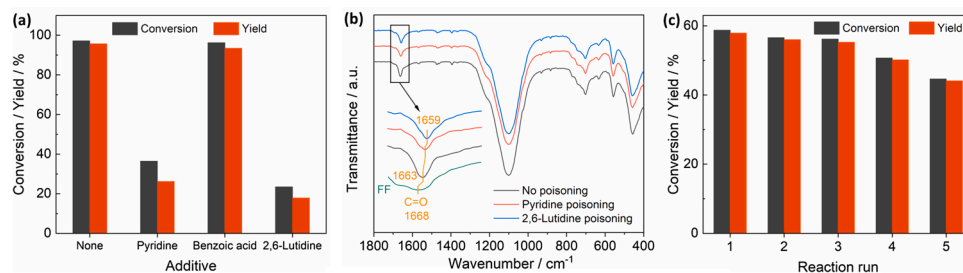
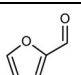
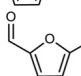
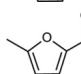
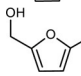


Fig. 4. (a) Acetalization of FF to FD with APO-5(1) with/without poisoning additives. Reaction conditions: FF (96 mg, 1 mmol), APO-5(1) (100 mg), additive (100 mg), EG (2 mL), 1,4-dioxane (3 mL), 150 °C, 24 h. (b) FT-IR spectra of FF, APO-5(1) with pre-adsorbed FF with/without poisoning additives. (c) Reusability of APO-5(1) in the conversion of FF to FD. Reaction conditions: FF (96 mg, 1 mmol), APO-5(1) (100 mg), EG (2 mL), 1,4-dioxane (3 mL), 150 °C, 24 h.

Table 3
Acetalization of various aldehydes with APO-5(1) catalyst^a.

Entry	Substrate	Conv. (%) ^b	Yield (%) ^b	Yield (%) ^b
1		97.2	95.7	–
2		90.1	83.8	4.7
3		95.7	93.4	–
4		98.0	88.4	3.9

^a Reaction conditions: Substrate (1 mmol), APO-5(1) (100 mg), EG (2 mL), 1,4-dioxane (3 mL), 150 °C, 24 h.

^b Conversion and yield were quantified using ¹H NMR.

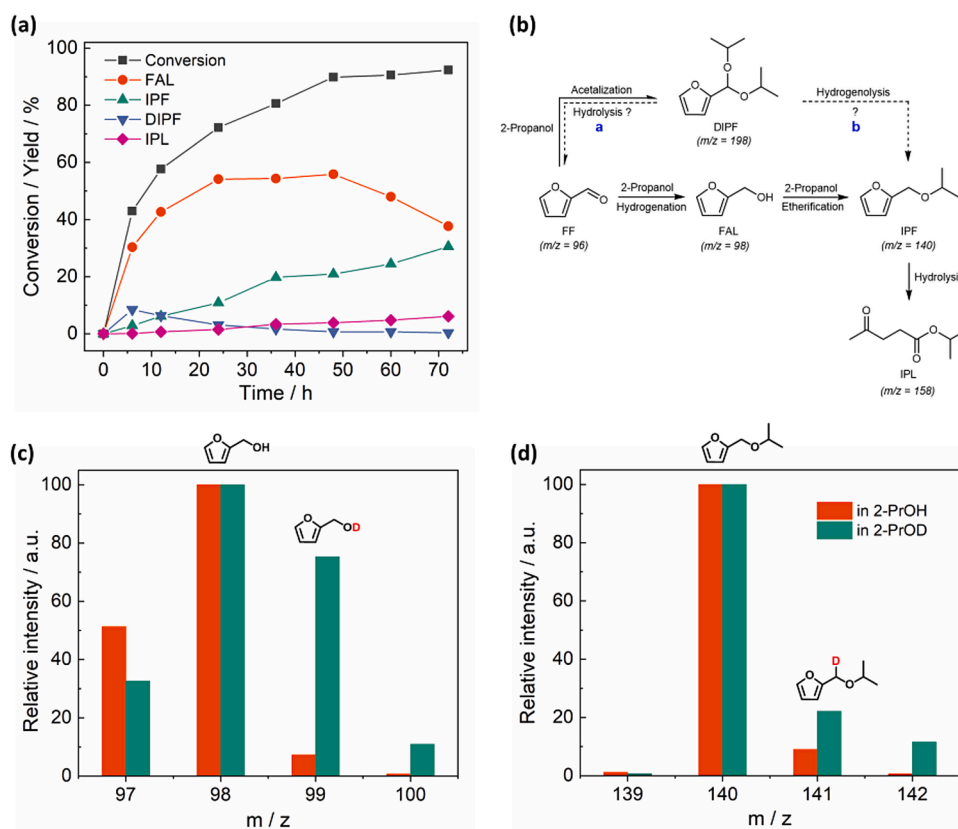


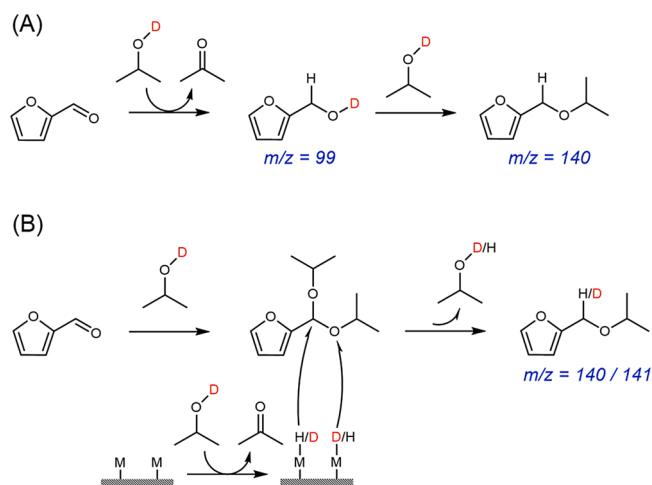
Fig. 5. (a) Time course of the reductive etherification of FF over APO-5(1.5). Reaction conditions: FF (96 mg, 1 mmol), APO-5(1.5) (100 mg), 2-propanol (5 mL), 120 °C. (b) Possible pathways for the reductive etherification of FF. (c) and (d) Results from GC-MS analysis of reaction products FAL and IPF after the reductive etherification of FF over APO-5(1.5). Reaction conditions: FF (96 mg, 1 mmol), APO-5(1.5) (100 mg), 2-propanol/ 2-propanol-OD (5 mL), 140 °C, 24 h.

3.4.2. Co-solvent and hydrogen donor study

Previous work has suggested 1,4-dioxane to be a beneficial co-solvent for etherification [50], and its influence was therefore also investigated here using various added amounts in 2-propanol (Fig. 6). In neat 1,4-dioxane (100 vol.%) only 5% of FF was converted and FAL, IPF and IPL products were not formed because 1,4-dioxane cannot transfer hydrogen to FF. With 40 vol.% 1,4-dioxane added the FF conversion and IPF yield were significantly enhanced providing an apparent optimal mixture for catalytic transfer hydrogenation and successive etherification. However, with lower amounts of added 1,4-dioxane the IPF yield decreased and the FAL yield increased, while the FF conversion and IPL yield remained almost constant. To confirm that 1,4-dioxane facilitated the etherification, FAL was used as substrate in 2-propanol

alone and in 40 vol.% 1,4-dioxane mixture. The results (Table S4, entries 1 and 2) revealed a higher IPF yield (12 %) in the mixed solvent than in 2-propanol alone, showing that the co-solvent indeed facilitated the etherification consistent with earlier observations for other etherification reactions [50]. Notably, the presence of minor amount of water significantly inhibited the catalyst and the conversion of FF and production of IPF (Table S4, entries 3 and 4). Since 1,4-dioxane is prone to form hydrogen bonds with water [51,52], it may infer that hydrogen bond formation between 1,4-dioxane and water prevented the catalyst inhibition and thereby facilitated the reaction.

The effect of the hydrogen donor on the reductive etherification of FF catalyzed by APO-5(1.5) was also investigated (Fig. S7). When primary alcohols (ethanol, 1-propanol, 1-butanol and isobutanol) were used as



Scheme 1. Two possible mechanisms for the formation of IPF from FF.

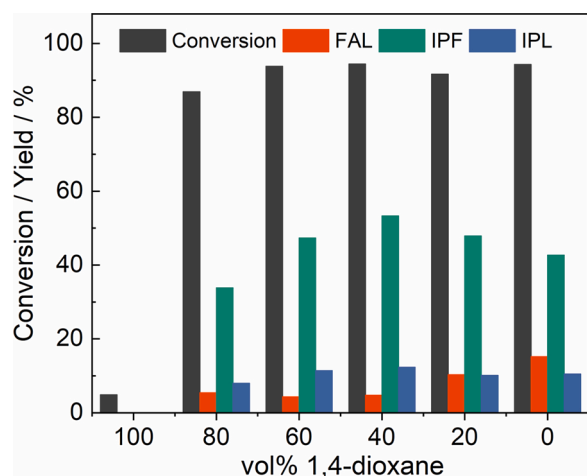


Fig. 6. The effect of 1,4-dioxane as co-solvent in the reductive etherification of FF over APO-5(1.5) in 2-propanol. Reaction conditions: FF (96 mg, 1 mmol), APO-5(1.5) (100 mg), solvent (5 mL), 140 °C, 24 h.

solvent and hydrogen donor, FF conversion and FAL selectivity were markedly lower than when using secondary alcohols (2-propanol and 2-butanol), confirming that secondary alcohols have a higher tendency to release hydrogen than primary alcohols [53]. In the 2-butanol system, both the FF conversion and FAE selectivity were lower than in 2-propanol while the FAL selectivity was higher, suggesting that steric hindrance of the solvent affected both the hydrogen transfer and the etherification.

3.4.3. Catalyst recycling study

Finally, the reusability of the APO-5(1.5) catalyst was investigated for the reductive etherification of FF (Fig. 7). After the initial reaction run and successive washing (acetone and methanol) and drying of the catalyst the performance altered in the next reaction run with lower FF conversion and IPF yield. Characterization of the reused catalyst by TG and N_2 physisorption analysis (Fig. S8 and Table S1, entry 3) revealed an increased weight loss (9.1 wt.%) as well as a drastically decreased surface area and pore volume compared to the fresh catalyst. Similarly, the FT-IR spectrum (Fig. S9) showed bands at around 2950 and 1400 cm^{-1} (C-H stretching and bending vibrations of CH_3 and CH_2), 1628 cm^{-1} (C=C stretching vibrations) and 869 cm^{-1} which may be assigned to adsorbed 1,4-dioxane [45]. Combined this corroborated that the catalyst deactivation originated from adsorbed organic species blocking the

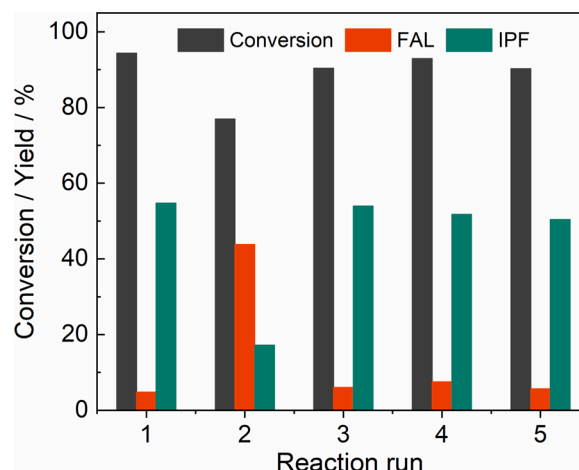


Fig. 7. Reusability of APO-5(1.5) in the reductive etherification of FF to IPF. Reaction conditions: FF (96 mg, 1 mmol), APO-5(1.5) (100 mg), 2-propanol (3 mL), 1,4-dioxane (2 mL), 140 °C, 24 h.

pores and lowering the accessibility of the substrates to the catalytically active sites like found for the APO-5(1) catalyst in the acetalization of FF to FD (see above). Moreover, the adsorbed species likely slowed down the reaction, which resulted in a different product distribution for FAL and IPF compared to the initial reaction run. Intermediate calcination (550 °C, 1 h) of the catalyst, allowed removing the adsorbed species and restore the original catalyst performance in three consecutive reaction runs. Importantly, the XRD pattern of the reused catalyst after five recycles was identical to the fresh catalyst (Fig. S10), clearly suggesting that the catalyst structure remained stable upon the thermal treatment and that the catalyst system was highly durable.

4. Conclusions

Hydrothermally synthesized APO-5s (Al/P = 1, 1.25 and 1.5) were applied as catalysts in the acetalization and reductive etherification of FF. The materials had lower crystallinity with higher Al content but larger surface area, pore volume and acidity, and these characteristics facilitated high catalyst selectivity in the valorization of FF into FAs and FAEs, respectively. Hence, APO-5(1) provided an excellent yield of 96 % of the cyclic acetal FD in EG/1,4-dioxane, and a low degree of catalyst deactivation after five recycles correlated to pore blocking by adsorbed organic species. Similarly, high catalyst activity was shown with alternative furanic carbonyl compounds and longer chained diols. Furthermore, poisoning experiments suggested that Brønsted acid sites of the catalyst dominated the acetalization performance, whereas pre-adsorption experiments with FF supported that adsorption and acidic sites co-catalyzed the reaction. On the other hand, APO-5(1.5) provided good performance in the reductive etherification of FF in 2-propanol yielding 55 % of IPF. The pathway for direct hydrogenolysis of acetal by hydrogen transfer by 2-propanol as a hydrogen donor was investigated, and the addition of 1,4-dioxane was shown to improve the etherification, possibly due to hydrogen bond formation between 1,4-dioxane and the formed water. The APO-5(1.5) catalyst deactivated more severely than APO-5(1) after reuse, but intermediate calcination completely regained the initial catalyst performance and left the catalyst structure intact.

The work demonstrates a simple approach to design heterogeneous APO catalyst systems for the efficient and highly selective valorization of biomass-derived FF to attractive fuel bio-additives. Future work should focus on product separation and evaluate the potential for industrial implementation.

CRediT authorship contribution statement

Wenting Fang: Methodology, Investigation, Writing - original draft, Visualization. **Anders Riisager:** Conceptualization, Validation, Writing - review & editing.

Declaration of Competing Interest

The authors declare that they have no known competing financial interests or personal relationships that could have appeared to influence the work reported in this paper.

Acknowledgements

W.F. acknowledges the China Scholarship Council (No. 201908330324) for awarding a scholarship and the Department of Chemistry, Technical University of Denmark is acknowledged for supporting the work.

Appendix A. Supplementary data

Supplementary data associated with this article can be found, in the online version, at <https://doi.org/10.1016/j.apcatb.2021.120575>.

References

- [1] A.R. Trifoi, P.Ş. Agachi, T. Pap, *Renew. Sustain. Energy Rev.* 62 (2016) 804–814.
- [2] O.M. Ali, R. Mamat, C.K.M. Faizal, *J. Renew. Sustain. Energy* 5 (2013).
- [3] C.J.A. Mota, C.X.A. da Silva, N. Rosenbach, J. Costa, F. da Silva, *Energy Fuel* 24 (2010) 2733–2736.
- [4] A. Cornejo, I. Barrio, M. Campoy, J. Lázaro, B. Navarrete, *Renew. Sustain. Energy Rev.* 79 (2017) 1400–1413.
- [5] R. Mariscal, P. Mairesles-Torres, M. Ojeda, I. Sádaba, M. López Granados, *Energy Environ. Sci.* 9 (2016) 1144–1189.
- [6] B.L. Wegenhart, S. Liu, M. Thom, D. Stanley, M.M. Abu-Omar, *ACS Catal.* 2 (2012) 2524–2530.
- [7] K.S. Arias, A. Garcia-Ortiz, M.J. Climent, A. Corma, S. Iborra, *ACS Sustain. Chem. Eng.* 6 (2018) 4239–4245.
- [8] D.R. Chaffey, T.E. Davies, S.H. Taylor, A.E. Graham, *ACS Sustain. Chem. Eng.* 6 (2018) 4996–5002.
- [9] V.E. Tarabanko, M.Y. Chernyak, I.L. Simakova, K.L. Kaigorodov, Y.N. Bezborodov, N.F. Orlovskaya, *Russ. J. Appl. Chem.* 88 (2016) 1778–1782.
- [10] J.P. Lange, E. van der Heide, J. van Buijtenen, R. Price, *ChemSusChem* 5 (2012) 150–166.
- [11] E.V. Gromachevskaya, F.V. Kvitkovsky, E.B. Usova, V.G. Kulnevich, *Chem. Heterocycl. Comp.* 40 (2004) 979–985.
- [12] S.P. Gavriiova, T.G. Serkina, L.A. Badovskaya, *Chem. Heterocycl. Comp.* 29 (1993) 268–270.
- [13] Hartati, D. Prasetyoko, M. Santoso, *Indones. J. Chem.* 16 (2016) 289–296.
- [14] B. Mallesham, P. Sudarsanam, B.M. Reddy, *Catal. Sci. Technol.* 4 (2014) 803–813.
- [15] A. Patil, S. Shinde, S. Kamble, C.V. Rode, *Energy Fuel* 33 (2019) 7466–7472.
- [16] T.A. Natsir, T. Hara, N. Ichikuni, S. Shimazu, *ACS Appl. Energy Mater.* 1 (2018) 2460–2463.
- [17] M. Paniagua, J.A. Melero, J. Iglesias, G. Morales, B. Hernandez, C. Lopez-Aguado, *Appl. Catal. A: Gen.* 537 (2017) 74–82.
- [18] M. Tian, R.L. McCormick, J. Luecke, E. de Jong, J.C. van der Waal, G.P.M. van Klink, M.D. Boot, *Fuel* 202 (2017) 414–425.
- [19] C.R. Patil, C.V. Rode, *ChemistrySelect* 3 (2018) 12504–12511.
- [20] M.M. Antunes, S. Lima, P. Neves, A.L. Magalhaes, E. Fazio, A. Fernandes, F. Neri, C. M. Silva, S.M. Rocha, M.F.R. Eiro, M. Pillinger, A. Urakawa, A.A. Valente, *J. Catal.* 329 (2015) 522–537.
- [21] M.M. Antunes, S. Lima, P. Neves, A.L. Magalhaes, E. Fazio, F. Neri, M.T. Pereira, A. F. Silva, C.M. Silva, S.M. Rocha, M. Pillinger, A. Urakawa, A.A. Valente, *Appl. Catal. B: Environ.* 182 (2016) 485–503.
- [22] S.P. Elangovan, V. Krishnasamy, V. Murugesan, *Catal. Lett.* 36 (1996) 271–277.
- [23] T. Muñoz, A.M. Prakash, L. Kevan, K.J. Balkus, *J. Phys. Chem. B* 102 (1998) 1379–1386.
- [24] L. Zhou, T. Lu, J. Xu, M. Chen, C. Zhang, C. Chen, X. Yang, J. Xu, *Microporous Mesoporous Mater.* 161 (2012) 76–83.
- [25] S.D. Ponja, I.P. Parkin, C.J. Carmalt, *RSC Adv.* 6 (2016) 102956–102960.
- [26] X. Zhao, X. Zhang, Z. Hao, X. Gao, Z. Liu, J. Porous. Mater. 25 (2017) 1007–1016.
- [27] M. Wang, Z. Wang, S. Liu, R. Gao, K. Cheng, L. Zhang, G. Zhang, X. Min, J. Kang, Q. Zhang, Y. Wang, *J. Catal.* 394 (2021) 181–192.
- [28] Tetsuya Kodaira, Kohji Miyazawa, Takujilkeda, Y. Kiyozumi, *Microporous Mesoporous Mater.* 29 (1999) 329–337.
- [29] S.H. Jung, Y.K. Hwang, J.-S. Chang, S.-E. Park, *Microporous Mesoporous Mater.* 67 (2004) 151–157.
- [30] S.H. Jung, J.S. Chang, Y.K. Hwang, S.E. Park, *J. Mater. Chem.* 14 (2004) 280–285.
- [31] B. Chen, C.W. Kirby, Y. Huang, *J. Phys. Chem. C* 113 (2009) 15868–15876.
- [32] C.A. Fyfe, K.C. Wong-Moon, Y. Huang, *Zeolites* 16 (1996) 50–55.
- [33] N. Sheng, Y.Y. Chu, S.H. Xing, Q. Wang, X.F. Yi, Z.C. Feng, X.J. Meng, X.L. Liu, F. Deng, F.S. Xiao, *J. Am. Chem. Soc.* 138 (2016) 6171–6176.
- [34] L.S. de Saldarriaga, C. Saldarriaga, M.E. Davis, *J. Am. Chem. Soc.* 109 (1987) 2686–2691.
- [35] Z. Yan, B. Chen, Y. Huang, *Solid State Nucl. Magn.* 35 (2009) 49–60.
- [36] A. Sayari, I. Moudrakovski, J.S. Reddy, C.I. Ratcliffe, J.A. Ripmeester, K.F. Preston, *Chem. Mater.* 8 (1996) 2080–2088.
- [37] L. Gomez-Hortigueela, C. Marquez-Alvarez, F. Cora, F. Lopez-Arbeloa, J. Perez-Pariente, *Chem. Mater.* 20 (2008) 987–995.
- [38] S. Endud, N. Roslan, Z. Ramli, H.O. Lintang, *Adv. Mater. Res.* 1109 (2015) 360–364.
- [39] M. Zaarour, O. Perez, P. Boullay, J. Martens, B. Mihailova, K. Karaghiosoff, L. Palatinus, S. Mintova, *CrystEngComm* 19 (2017) 5100–5105.
- [40] X.-L. Li, K. Zhang, S.-Y. Chen, C. Li, F. Li, H.-J. Xu, Y. Fu, *Green Chem.* 20 (2018) 1095–1105.
- [41] M.R. Nanda, Y. Zhang, Z. Yuan, W. Qin, H.S. Ghaziaskar, C. Xu, *Renew. Sustain. Energy Rev.* 56 (2016) 1022–1031.
- [42] S.H. Zhou, F.L. Dai, Z.Y. Xiang, T. Song, D.T. Liu, F.C. Lu, H.S. Qi, *Appl. Catal. B: Environ.* 248 (2019) 31–43.
- [43] Y. Yang, L. Chen, Y. Chen, W. Liu, H. Feng, B. Wang, X. Zhang, M. Wei, *Green Chem.* 21 (2019) 5352–5362.
- [44] M. Ma, P. Hou, J. Cao, H. Liu, X. Yan, X. Xu, H. Yue, G. Tian, S. Feng, *Green Chem.* 21 (2019) 5969–5979.
- [45] F.E. Malherbe, H.J. Bernstein, *J. Am. Chem. Soc.* 74 (1952) 4408–4410.
- [46] M. Balakrishnan, E.R. Sacia, A.T. Bell, *Green Chem.* 14 (2012) 1626–1634.
- [47] H. Nguyen, N. Xiao, S. Daniels, N. Marcella, J. Timoshenko, A. Frenkel, D. G. Vlachos, *ACS Catal.* 7 (2017) 7363–7370.
- [48] E.R. Sacia, M. Balakrishnan, A.T. Bell, *J. Catal.* 313 (2014) 70–79.
- [49] Y. Wang, Q. Cui, Y. Guan, P. Wu, *Green Chem.* 20 (2018) 2110–2117.
- [50] K. Klepáčová, D. Mravec, A. Kaszonyi, M. Bajus, *Appl. Catal. A: Gen.* 328 (2007) 1–13.
- [51] K. Mizuno, S. Imafuji, T. Fujiwara, T. Ohta, Y. Tamiya, *J. Phys. Chem. B* 107 (2003) 3972–3978.
- [52] P. Borowski, W. Gac, P. Pulay, K. Woliński, *New J. Chem.* 40 (2016) 7663–7670.
- [53] D. Scholz, C. Aellig, I. Hermans, *ChemSusChem* 7 (2014) 268–275.